Block-based Compressive Sensing Coding of Natural Images by Local Structural Measurement Matrix

Xinwei Gao*, Jian Zhang†, Wenbin Che*, Xiaopeng Fan*, Debin Zhao*

*Harbin Institute of Technology
Harbin 150001, China
{xwgao.cs,chewenbin,fxp,dbzhao}@hit.edu.cn

†Peking University
Beijing 100871, China
jian.zhang@pku.edu.cn

Abstract

Gaussian random matrix (GRM) has been widely used to generate linear measurements in compressive sensing (CS) of natural images. However, in practice, there actually exist two problems with GRM. One is that GRM is non-sparse and complicated, leading to high computational complexity and high difficulty in hardware implementation. The other is that regardless of the characteristics of signal the measurements generated by GRM are also random, which results in low efficiency of compression coding. In this paper, we design a novel local structural measurement matrix (LSMM) for block-based CS coding of natural images by utilizing the local smooth property of images. The proposed LSMM has two main advantages. First, LSMM is a highly sparse matrix, which can be easily implemented in hardware, and its reconstruction performance is even superior to GRM at low CS sampling subrate. Second, the adjacent measurement elements generated by LSMM have high correlation, which can be exploited to greatly improve the coding efficiency. Furthermore, this paper presents a new framework with LSMM for block-based CS coding of natural images, including measurement generating, measurement coding and CS reconstruction. Experimental results show that the proposed framework with LSMM for block-based CS coding of natural images greatly enhances the existing CS coding performance when compared with other state-of-the-art image CS coding schemes.

1. Introduction

In recent years, Compressive Sensing (CS) has been extensively studied, whose purpose is to reconstruct the natural image from its observed measurements

$$y = \Phi x, \tag{1}$$

where $x \in R^N$ is lexicographically stacked representations of the original image and $y \in R^M$ is the CS measurements observed by a random $M \times N$ measurement matrix Φ, $(M \ll N)$. From many fewer acquired measurements than suggested by the Nyquist sampling theory, CS theory demonstrates that a signal can be reconstructed with high probability when it exhibits sparsity in some domain Ψ, which has greatly changed the way engineers think of data acquisition,

$$x = \Psi\theta. \tag{2}$$

If θ is a sparse coefficient vector, the signal x is sparse under the domain Ψ. In most CS literature, both sensing architectures [1] and image reconstruction algorithms [2–7] are proposed. Although CS measurement process can be regarded as a combination of image acquisition and image compression, this process is not a real compression in the strict information theoretic sense, because it cannot directly produce a bitstream from

1068-0314/15 $31.00 © 2015 IEEE
DOI 10.1109/DCC.2015.47

the sensing device hardware, which can be only seen as a technology of dimensionality reduction in essence [2].

As a very important technology of image coding, quantization is introduced into the CS image coding model [3], which is applied for each CS measurement. However, due to the random characteristic of generated measurements by the random matrix Φ, isometric scalar quantization does not perform well in rate-distortion performance.

Inspired by the success of the block-based hybrid video coding, such as HEVC [8], H.264, MPEG-2, the inter prediction coding technology can be used in the CS measurement process. Some works [2, 4, 5] on the block-based CS (BCS) hybrid coding framework are presented. Mun and Fowler proposed the block-based quantized compressed sensing of natural images with differential pulse-code modulation (DPCM) [2] and uniform scalar quantization. In [2], the previous decoded measurement is taken as the candidate of the current measurement. Zhang et al. extended the DPCM based CS measurement coding and proposed the spatially directional predictive coding (SDPC) [4], in which the intrinsic spatial correlation between neighbouring measurements of natural images are further explored. In the BCS [9] measurement coding, Khanh et al. [5] points out that, the spatial correlation among neighboring blocks becomes higher as block size decreases and the CS recovery of a small block is less efficient than that of a large block. In order to balance the conflict between compressed ratio and reconstructed quality, a structural measurement matrix (SMM) is proposed [5] to achieves a better RD performance, in which the image is sampled by some small blocks, and reconstructed with large blocks spliced by the small block. However, all these above block-based hybrid CS coding frameworks [2, 4, 5] with Gaussian random matrix (GRM) only utilize the inter-block prediction to improve the RD performance. In the intra prediction of HEVC, it can be noticed that in the spatial domain the inter-block prediction between non-overlapped blocks is less efficient than the directional intra-block prediction using the nearby L line pixels. But in the measurement domain with GRM, regardless of the characteristics of signal the generated measurements by GRM are random, which results in low efficiency of prediction coding. Furthermore, GRM is a non-sparse and complicated matrix, leading to high computational complexity and high difficulty in hardware implementation.

In considering the above problems, we design a novel local structural measurement matrix (LSMM) for block-based CS coding of natural images by utilizing the local smooth property of images. The proposed LSMM has two main advantages. First, LSMM is highly sparse, which can be easily implemented in hardware, and its reconstruction performance is even superior to GRM at low CS sampling subrate. Second, the generated adjacent measurements with LSMM have high correlation, which can be exploited to greatly improve the coding efficiency. Furthermore, this paper presents a new framework with LSMM for block-based CS coding of natural images, including measurement generating, measurement coding and CS reconstruction. Experimental results show that the proposed framework with LSMM for block-based CS coding of natural images greatly enhances the existing CS coding performance when compared with other state-of-the-art image CS coding schemes.

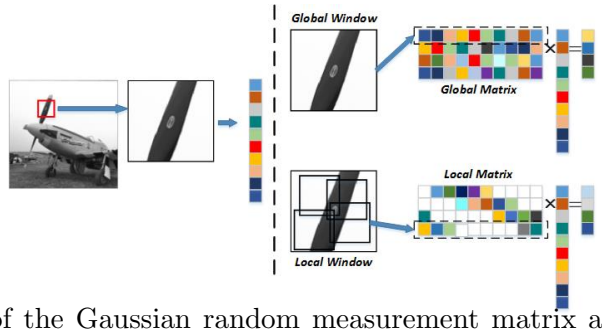

Figure 1: Diagram of the Gaussian random measurement matrix and the proposed local structural measurement matrix.

2. The Local Structural Measurement Matrix

As discussed in Section 1, the block-based CS coding schemes [2, 4, 5] of natural images with Gaussian random matrix (GRM) only utilize the inter-block correlation between non-overlapped neighbouring blocks, which results in high computational complexity and low coding efficiency. In order to further improve the coding efficiency with easy hardware implementation, we hope to design a new measurement matrix, which is not only sparse but also can generate CS measurements with high correlation. In our design, the new measurement matrix is based on the local smoothness characteristics of natural images, which is named as local structural measurement matrix (LSMM).The design details of LSMM are given below.

In this design, most of the random elements in the LSMM denoted by Φ are set to be zero, which makes the LSMM highly sparse for easy implementation. The kth line of the matrix Φ is denoted by $\Phi(k) = \{a_{k,1}, a_{k,2}, ..., a_{k,N_b}\}$, N_b is the number of pixels in one block. For the specific application of natural image compressive sensing coding, by considering the local smoothness characteristics of the image, these pixels in the image corresponding to these non-zero elements in the $\Phi(k)$ are composed of a local window. As shown in Fig. 1, with the GRM, an element of the measurement is computed as the random weighted sum of all the pixels in a block, but in ours design of LSMM, an element of the measurement is computed with the pixels in a corresponding local window. All the non-zero elements in $\Phi(k)$ are set to be positive and each $a_{k,i} = 0$ means its corresponding pixel is outside the kth local window in the image. The constraint of $\Phi(k)$ is:

$$\|\Phi(k)\|_0 = L^2, \quad a_{k,i} \geq 0 \quad and \quad \sum_{i=1}^{N_b} a_{k,i} = 1, \tag{3}$$

where the size of the local window is $L \times L$. Therefore the generated measurement is similar with these pixels in the corresponding local window. The reconstruction performances of GRM and the proposed LSMM with SPL-DCT [10] algorithm are demonstrated by the experiment. As shown in Table. 1, compared with GRM, LSMM is particularly effective at the low CS sampling subrate, and does not perform well at the high CS sampling subrate. It is noteworthy that, LSMM is very suitable for the application of image CS coding, because image CS coding does not usually use a too high sampling subrate in practice.

Table 1: The uncompressed CS reconstruction performance (PSNR) by SPL-DCT with GRM and LSMM.

Sampling subrate	*Airplane*		*Monarch*		*Parrot*		*Peppers*	
	GRM	LSMM	GRM	LSMM	GRM	LSMM	GRM	LSMM
0.05	23.61	**24.38**	20.48	**22.49**	26.15	**27.46**	25.06	**26.01**
0.10	25.54	**26.48**	23.12	**25.39**	28.15	**29.73**	27.90	**29.26**
0.15	27.07	**27.60**	24.88	**26.62**	29.39	**30.81**	28.56	**30.93**
0.20	27.06	**28.51**	26.43	**28.20**	30.40	**32.38**	29.30	**32.09**
0.25	29.09	**29.20**	27.62	**28.95**	31.48	**33.17**	29.87	**32.72**
0.30	**30.00**	29.68	28.84	**29.48**	32.52	**33.72**	31.01	**33.04**
0.35	**30.92**	29.98	29.62	**29.79**	33.53	**33.54**	31.71	**32.86**
0.40	**31.77**	30.62	**30.61**	30.57	**34.28**	34.77	33.81	**33.81**
0.45	**32.61**	30.97	**31.40**	30.95	**35.32**	35.21	**34.44**	34.14
0.50	**33.68**	31.36	**32.22**	31.32	**36.45**	35.76	**35.07**	34.40

Because the nearby pixels are similar in the image and the measurement is similar with these pixels in the corresponding local window, the neighboring measurements are also similar with each other. The generated adjacent measurements with high correlation can be exploited to greatly improve the coding efficiency. As we know, edges and other structured high-frequency features of natural images are very important to perceptual quality. The LSMM can be seen as a broad-band filter and it retains the correlation between these neighboring CS measurements and hence leaves the CS measurement coding the possibility of getting higher compression rate. To demonstrate the superiority of the proposed LSMM over GRM, a further quantitative comparison will be provided in the next section.

3. The Proposed Image CS Coding Framework

In the block-based hybrid CS coding framework, the input natural image is divided into non-overlapped blocks and these blocks are linear projected by the same Gaussian random matrix (GRM). At the encoder, each current measurement of a block is coded by the prediction measurement. In DPCM based CS measurement coding [2], the prediction measurement is the decoded measurement of the previous block; In SDPC [4], the optimal prediction measurement is selected from a set of candidates that are generated by four designed directional predictive modes. Then, the prediction residuals are uniform scalar quantized and entropy encoded into bitstreams. The decoder process is the inverse of encoder.

In the proposed image CS coding framework, the local smoothness characteristics of the image is utilized by the block-based local structural measurement matrix (LSMM) Φ. An image is divided into non-overlapped blocks, each measurement of a block is observed by the same matrix Φ. The measurement of kth block is defined as $M_k = \{m_{k,1}, m_{k,2}, ..., m_{k,N_e}\}$, N_e is the number of elements in a measurement. By LSMM, each observed element of the measurement in a local window is highly related with those in nearby local windows. The first element $m_{k,1}$ of M_k in the kth block is directly scalar-quantized and entropy coded into bitstreams. At the process of coding the ith element $m_{k,i}$, the prediction candidate is selected by the shortest Euclidean

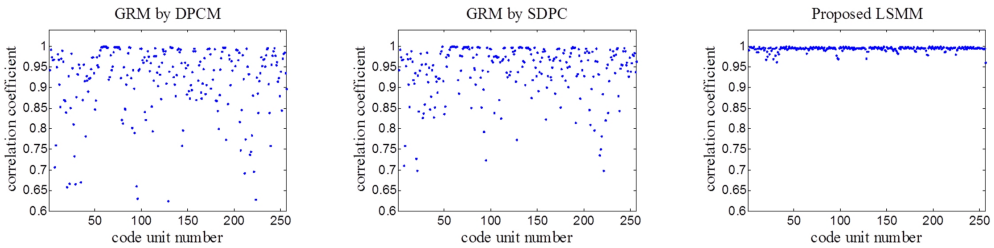

Figure 2: Three types of correlation coefficients (DPCM by GRM, SDPC by GRM and the proposed LSMM) on the test image *Peppers* with the sampling subrate = 0.25 and the block size for BCS is 32×32.

distance between the local window of $m_{k,i}$ and those windows of previous decoded element in M_k. The prediction element, denoted by $\hat{m}_{k,i}$, after obtaining the prediction $\hat{m}_{k,i}$ of $m_{k,i}$, the residuals $r_{k,i}$ can be calculated by $r_{k,i} = m_{k,i} - \hat{m}_{k,i}$, then $r_{k,i}$ is scalar-quantized and entropy coded into bitstreams. To demonstrate the superiority of the proposed LSMM over GRM, we make a further quantitative comparison. All the ith elements of measurements in all non-overlapped blocks are composed as an unit named G_i, the corresponding prediction unit is define as $\hat{G}_i$. Like [5], the correlation coefficient to measure the correlation of an unit and the corresponding prediction unit is shown by

$$\rho\left(G_i, \hat{G}_i\right) = \frac{G_i^T \hat{G}_i}{\|G_i\|_2 \left\|\hat{G}_i\right\|_2}, \tag{4}$$

where the correlation coefficient is defined as ρ. It can be seen in Fig. 2, correlation coefficients of coding units by LSMM are much higher than these two correlation coefficients of DPCM coding units and SDPC coding units by GRM.

At the decoder, by the de-quantization on quantizer indexes from the bitstream the quantized residuals $\tilde{r}_{k,i}$ can be obtained, which is then added by the prediction $\hat{m}_{k,i}$, producing the reconstructed CS measurements group $\tilde{m}_{k,i} = \tilde{r}_{k,i} + \hat{m}_{k,i}$, ready for further prediction coding. At last, all groups of reconstructed measurements $\tilde{y}$ are obtained sequentially, which are then utilized for the natural image reconstruction by CS recovery algorithms. Compressive sensing theory allows that a natural image x can be exactly recovered from its space measurements y acquired by linear projection with the sampling subrate $S = M/N$, if x has advantage of being sparse in a domain, e.g. DCT domain, DWT domain, or some incoherent domains. Different from other signals, natural image as a two-dimensional signal has its own prior knowledge, such as local smoothing model and group sparse model. To cope with the ill-posed problem of natural image CS recovery, these traditional methods employ various image prior knowledge for regularizing the solution to the following minimization problem:

$$argmin_x \frac{1}{2} \|y - \Phi x\|_2^2 + \lambda \Gamma(x), \tag{5}$$

where y is the observed measurement value at the encoder, $\frac{1}{2}\|y - \Phi x\|_2^2$ is the l_2-norm data-fidelity term, $\Gamma(x)$ is called the regularization term denoting image prior and λ is the regularization parameter. Due to that image prior knowledge plays an important role in the performance of the uncompressed image CS restoration algorithms, designing effective regularization terms $\Gamma(x)$ to reflect the image priors

is at the core of image restoration. Some image prior models are usually used as the regularization term, such as the local smoothing based total variation (TV) model [11], nonlocal self-similarity [12] based model and these dictionary based models: DCT model, DWT model and KSVD [13] model. However, in the case of image CS restoration with compressed measurements, the true measurements y does not exist in the decoder, the instead l_2 data-fidelity term $\frac{1}{2}\|\tilde{y}-\Phi x\|_2^2$ cannot accurately reflect the accuracy of the actual measurements value. Because the decoded measurements value $\tilde{y}$ reconstructed at the decoder by the sum of the predicted measurements and the quantized residual is not equal to the observed measurement value y at the encoder.

To deal with this problem, we propose a soft image compressive sensing reconstruction method with compressed measurements, in which the side information in the coded bitstreams is incorporated to confine the solution space and help to improve the restoration performance. For each decoded measurement $\tilde{y_i}=\hat{y_i}+\tilde{r_i}$, y_i being the corresponding actual measurement value and Q_S being the quantization step for the residual $\tilde{r_i}$, the quantization interval from the side information in bitstream for y_i:

$$y_i^{low} \le y_i < y_i^{up}, \tag{6}$$

where $y_i^{low}=\lfloor(\tilde{y_i}-\hat{y_i})/Q_S\rfloor Q_S+\hat{y_i}$ and $y_i^{up}=\lfloor(\tilde{y_i}-\hat{y_i})/Q_S+1\rfloor Q_S+\hat{y_i}$ are the lower and upper bounds of y_i. Here, $\le$ and $<$ denote the operation of element-wise comparison. The inequality can be incorporated into Eq.(5) to further refine the solution space and improve the performance. Finally, we formulate our problem of soft decoding as the following minimization problem:

$$argmin_x \frac{1}{2}\|F(\Phi x,\tilde{y},\hat{y},Q_S)\|_2^2+\lambda\Gamma(x), \tag{7}$$

$$F_i(\Phi(i)x,\tilde{y_i},\hat{y_i},Q_S)=\begin{cases}0 & \text{if } y_i^{low}\le\Phi(i)x<y_i^{up}\\ \tilde{y_i}-\Phi(i)x & \text{else}\end{cases}. \tag{8}$$

Then the general solution to this problem is given by adopting the framework of split Bregman iteration [14] (SBI). This minimization problem can be translated into an equivalent constrained optimization problem by introducing variables u and v:

$$argmin_{u,v}=\frac{1}{2}\|F(\Phi u,\tilde{y},\hat{y},Q_S)\|_2^2+\lambda\Gamma(v)\quad s.t.\quad u=v. \tag{9}$$

Algorithm 1 Generalized solution for Eq.(9) by split Bregman iteration.

Input:

Set μ, initialize $u^{(0)}$, $v^{(0)}$ and $z^{(0)}$, $t=0$;

1: **while** (stopping criterion is not satisfied) **do**

2: $u^{(t+1)}=argmin_u\frac{1}{2}\|F(\Phi u,\tilde{y},\hat{y},Q_S)\|_2^2+\frac{\mu}{2}\left\|u-v^{(t)}-z^{(t)}\right\|_2^2$;

3: $v^{(t+1)}=argmin_v\lambda\Gamma(v)+\frac{\mu}{2}\left\|u^{(t+1)}-v-z^{(t)}\right\|_2^2$; ;

4: $z^{(t+1)}=z^{(t)}-\left(u^{(t+1)}-v^{(t+1)}\right)\quad and\quad t=t+1$;

5: **end while**

So in this case the SBI addresses the minimization problem Eq. (9) into u sub-problem and v sub-problem as shown in Algorithm 1. Given $z^{(t)}$ and $v^{(t)}$, the u sub-problem is essentially a minimization problem of strictly convex quadratic function, that is

$$u=argmin_u\frac{1}{2}\|F(\Phi u,\tilde{y},\hat{y},Q_S)\|_2^2+\frac{\mu}{2}\left\|u-v^{(t)}-z^{(t)}\right\|_2^2. \tag{10}$$

Figure 3: All experimental test images.

The steepest gradient descent method is utilized to solve Eq. (10):

$$\tilde{u} = u - \gamma \frac{\partial \frac{1}{2} \left\| F\left(\Phi u, \tilde{y}, \hat{y}, Q_S\right) \right\|_2^2 + \frac{\mu}{2} \left\| u - v^{(t)} - z^{(t)} \right\|_2^2}{\partial u}, \tag{11}$$

where γ represents the optimal step. Therefore, solving u sub-problem only requires computing the following equation iteratively

$$\tilde{u} = u - \gamma \left(\Phi^T F\left(\Phi u, \tilde{y}, \hat{y}, Q_S\right) - \Phi^T \tilde{y} + \mu \left(u - v^{(t)} - z^{(t)} \right) \right), \tag{12}$$

where $\Phi^T \tilde{y}$, $\lfloor (\tilde{y}_i - \hat{y}_i) / Q_S \rfloor Q_S + \hat{y}_i$ and $\lfloor (\tilde{y}_i - \hat{y}_i) / Q_S + 1 \rfloor Q_S + \hat{y}_i$ can be calculated before, making above computation more efficient. The solution of the v sub-problem is dependent on the regularization term $\Gamma(v)$. If $\Gamma(v)$ is l_2-norm regularization term, it has the close form solution by least square method, else if $\Gamma(v)$ is l_1-norm or l_0-norm regularization term, the above minimization problem is large-scale and highly non-convex. Some approximation approaches, such as TV [11], K-SVD [13] and GSR [15], have been proposed to solve this l_1-norm or l_0-norm problem. It can be notice that each sub-problem minimization may be much easier than the original problem Eq.(5). In fact, we acquire the efficient solution for each separated sub-problem, which enables the whole soft decoding algorithm more efficient.

4. Experimental Results

In this section, we present experimental results of block-based CS coding of natural images by LSMM, and compare our results to some representative techniques in the literature: DPCM [2] and SDPC [4]. The image reconstruction algorithm are SPL-DCT [10] and GSR [15] separately. All the experimental test images are shown in Fig. 3, these natural images are of size 512×512 and the block size of BCS is set to be 32×32. The window size $L \times L$ of the LSMM is set to be 3×3. Following [2, 4, 5], the actual bitrate is estimated using the zero order entropy of the quantizer indexes, which can be actually produced by a real entropy coder. In all cases, for the experiments, the optimal combination of quantization step and sampling subrate is chosen via an exhaustive search over all combination pairs drawn from a finite set of quantization step and a finite set of sampling subrate. The rate-distortion performance in PSNR in dB and bitrate in bpp is provided in Fig. 4. The proposed LSMM achieves the highest PSNR over all the cases. By the SPL-DCT algorithm, the proposed LSMM can improve roughly more than 3.5dB and 3dB on average in comparison with GRM-DPCM and GRM-SDPC under the different bitrates on 0.3bpp, 0.6bpp and 0.9bpp. By the GSR algorithm, the performance of LSMM is 3dB and 2.5dB higher than GRM-DPCM and GRM-SDPC under the different bitrates on 0.3bpp, 0.6bpp and 0.9bpp. The reconstruction algorithm GSR achieves 3dB higher performances on

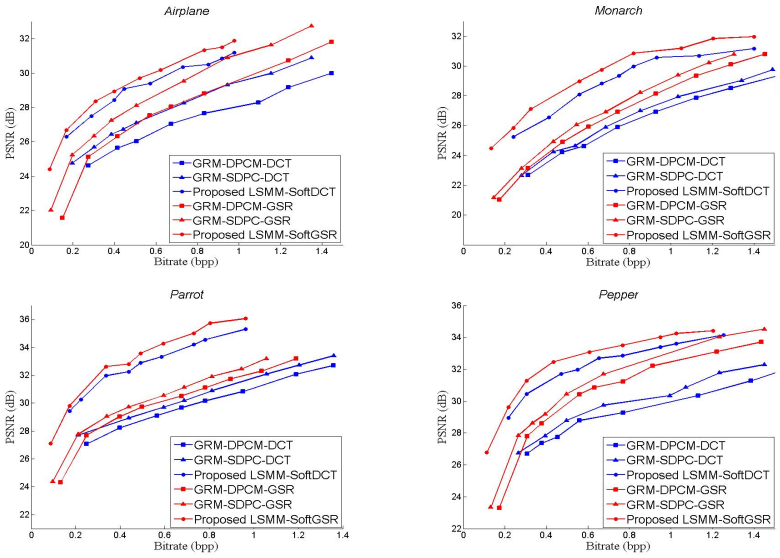

Figure 4: The rate-distortion performance on test images.

Table 2: The rate-distortion performances by different quantization step with DPCM, SDPC and LSMM with the sample-rate=0.25 using SPL-DCT reconstruction algorithm.

	0.4 bpp			0.5 bpp			0.6 bpp		
Pictures	DPCM	SDPC	LSMM	DPCM	SDPC	LSMM	DPCM	SDPC	LSMM
Airplane	22.24	24.69	**29.22**	24.31	26.74	**29.37**	25.35	27.45	**29.43**
Monarch	22.26	24.11	**29.64**	23.68	25.01	**28.97**	24.93	25.78	**29.10**
Parrot	26.13	27.85	**33.05**	27.74	29.05	**33.25**	29.10	29.68	**33.31**
Peppers	22.94	26.47	**31.82**	25.12	27.01	**32.55**	26.92	27.35	**32.64**
avg	23.39	25.87	**30.93**	25.21	26.95	**31.03**	26.57	27.56	**31.12**

average than SPL-DCT with the same coded CS measurements.

Then, we take the sampling subrate=0.25 as an example to show the rate-distortion performances by different quantization step with GRM-DPCM, GRM-SDPC and LSMM-SoftDecoding in Table 2 and Table 3. Compared with GRM-DPCM and GRM-SDPC, the proposed coding algorithm can improve roughly more than 5dB, 4dB, and 3dB on 0.4bpp, 0.5bpp and 0.6bpp by SPL-DCT, and improve 4dB, 3dB, and 1.5dB on 0.4bpp, 0.5bpp and 0.6bpp by GSR. Table 4 shows the performance comparison with the traditional reconstruction algorithms (DCT and GSR) and the proposed soft reconstruction algorithm (SoftDCT and SoftGSR) with LSMM. SoftDCT and SoftGSR can improve about 0.2dB and 0.3dB on average at the low bitrate about 0.2bpp. However at the middle bitrate and high bitrate, the quantization interval of the code measurement is very small, the performances of SoftDCT and SoftGSR are little higher than DCT and GSR. Finally, the subjective quality performances are shown in Fig. 5, it can be seen that, on the almost same bitrate, the images produced by LSMM are more clear than these by DPCM and SDPC, and the images produced with SoftDCT and SoftGSR are better than these with DCT and GSR.

Table 3: The rate-distortion performances by different quantization step with DPCM, SDPC and LSMM with the sampling subrate=0.25 using GSR reconstruction algorithm.

	0.4 bpp			0.5 bpp			0.6 bpp		
Pictures	DPCM	SDPC	LSMM	DPCM	SDPC	LSMM	DPCM	SDPC	LSMM
Airplane	22.54	26.13	**29.58**	25.74	28.21	**29.69**	26.05	29.76	**30.02**
Monarch	23.04	24.16	**29.47**	25.34	26.31	**29.77**	26.30	27.38	**29.89**
Parrot	27.05	29.20	**33.22**	28.98	31.22	**33.29**	31.32	32.20	**33.34**
Peppers	23.22	26.78	**32.61**	26.04	27.75	**32.94**	27.62	30.30	**33.02**
avg	23.96	26.56	**31.22**	26.52	28.37	**31.42**	27.82	29.91	**31.56**

Table 4: The rate-distortion performances of the traditional reconstruction algorithm and the proposed soft reconstruction algorithm of LSMM with the sampling subrate=0.25.

Pictures	DCT	SoftDCT	GSR	SoftGSR	bpp	DCT	SoftDCT	GSR	SoftGSR	bpp
Airplane	27.06	**27.15**	27.10	**27.39**	0.1499	29.05	**29.06**	29.42	**29.56**	0.3336
Monarch	27.34	**27.51**	27.82	**28.03**	0.2591	28.97	**28.98**	29.77	**29.86**	0.5054
Parrot	29.49	**29.84**	30.01	**30.38**	0.1926	32.71	**32.79**	33.02	**33.20**	0.3329
Peppers	29.47	**29.79**	30.30	**30.61**	0.2226	32.22	**32.34**	32.91	**32.92**	0.4542

5. Conclusion

In this paper, a novel local structural measurement matrix (LSMM) for block-based CS coding of natural images is proposed by utilizing the local smooth property of images, which has two main advantages compared with the Gaussian random matrix (GRM). Furthermore, a new framework with LSMM is presented for block-based CS coding of natural images, including measurement generating, measurement coding and CS reconstruction. Experimental results show that the proposed framework with LSMM for block-based CS coding of natural images greatly enhances the existing performance when compared with other state-of-the-art image CS coding schemes.

6. Acknowledgments

This work was supported in part by the Major State Basic Research Development Program of China (973 Program 2015CB351804), the National Natural Science Foundation of China under Grant No. 61272386, No. 61472101 and No. 61322106, the Program for New Century Excellent Talents in University of China (NCET-11-0797) and the Fundamental Research Funds for the Central Universities (Grant No. HIT.BRETIII.201221).

References

[1] M. Duarte, M. Davenport, D. Takhar, J. Laska, T. Sun, K. Kelly, and R. Baraniuk, "Single-pixel imaging via compressive sampling," *Signal Processing Magazine, IEEE*, vol. 25, no. 2, pp. 83–91, 2008.

[2] S. Mun and J. E. Fowler, "DPCM for quantized blockbased compressed sensing of images," in *Proc. of the Euro. Signal Process. Conf*, 2012, pp. 1424–1428.

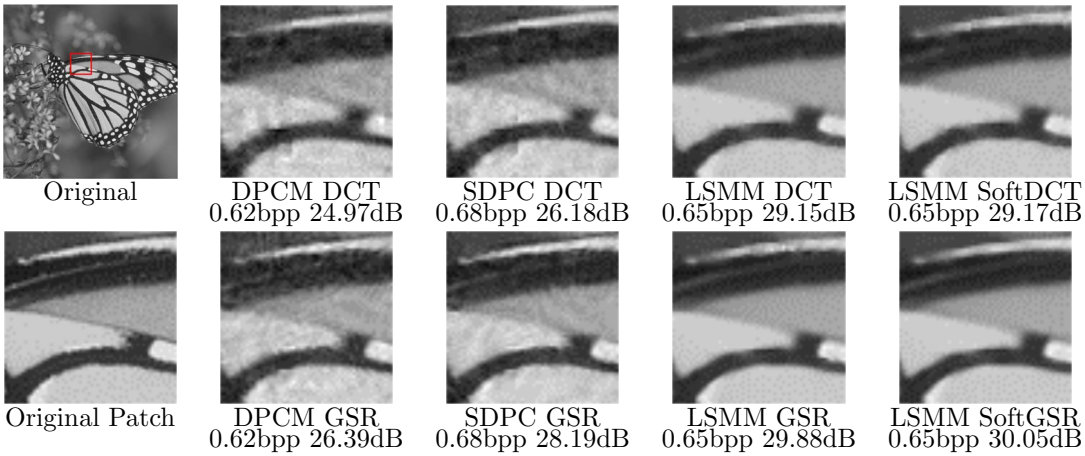

Figure 5: Visual quality comparison on test image *Monarch* with the sampling subrate=0.25.

[3] V. K. Goyal, A. K. Fletcher, and S. Rangan, "Compressive sampling and lossy compression," *Signal Processing Magazine, IEEE*, vol. 25, no. 2, pp. 48–56, 2008.

[4] J. Zhang, D. Zhao, and F. Jiang, "Spatially directional predictive coding for block-based compressive sensing of natural images," *IEEE International Conference on Image Processing*, pp. 1021–1025, 2013.

[5] K. Q. Dinh, H. J. Shim, and B. Jeon, "Measurement coding for compressive imaging using a structural measuremnet matrix," *IEEE International Conference on Image Processing*, pp. 10–13, 2013.

[6] J. Zhang, D. Zhao, C. Zhao, R. Xiong, S. Ma, and W. Gao, "Compressed sensing recovery via collaborative sparsity," in *Data Compression Conference (DCC), 2012*. IEEE, 2012, pp. 287–296.

[7] J. Zhang, D. Zhao, F. Jiang, and W. Gao, "Structural group sparse representation for image compressive sensing recovery," in *Data Compression Conference (DCC), 2013*. IEEE, 2013, pp. 331–340.

[8] G. J. Sullivan, J. Ohm, W. J. Han, and T. Wiegand, "Overview of the high efficiency video coding (HEVC) standard," *Circuits and Systems for Video Technology, IEEE Transactions on*, vol. 22, no. 12, pp. 1649–1668, 2012.

[9] L. Gan, "Block compressed sensing of natural images," in *Digital Signal Processing, 2007 15th International Conference on*, 2007, pp. 403–406.

[10] S. Mun and J. E. Fowler, "Block compressed sensing of images using directional transforms," in *IEEE International Conference on Image Processing*, 2009, pp. 3021–3024.

[11] A. Chambolle, "An algorithm for total variation minimization and applications," *Journal of Mathematical imaging and vision*, vol. 20, no. 1-2, pp. 89–97, 2004.

[12] M. Jung, X. Bresson, T. F. Chan, and L. A. Vese, "Nonlocal Mumford-Shah regularizers for color image restoration," *Image Processing, IEEE Transactions on*, vol. 20, no. 6, pp. 1583–1598, 2011.

[13] M. Aharon, M. Elad, and A. Bruckstein, "K-SVD: An algorithm for designing overcomplete dictionaries for sparse representation," *Signal Processing, IEEE Transactions on*, vol. 54, no. 11, pp. 4311–4322, 2006.

[14] T. Goldstein and S. Osher, "The split Bregman method for L1-regularized problems," *SIAM Journal on Imaging Sciences*, vol. 2, no. 2, pp. 323–343, 2009.

[15] J. Zhang, D. Zhao, and W. Gao, "Group-based sparse representation for image restoration," *Image Processing, IEEE Transactions on*, vol. 23, no. 8, pp. 3336–3351, 2014.